CHAPTER 8. QUANTITATIVE GEOLOGICAL SURFACE PROCESSES EXTRACTED FROM INFRARED SPECTROSCOPY AND REMOTE SENSING

Michael S. Ramsey,
Department of Geology and Planetary Science,
University of Pittsburgh,
Pittsburgh, Pennsylvania, 15260
ramsey@ivis.eps.pitt.edu

INTRODUCTION

Since its launch in December 1999, the Advanced Spaceborne Thermal Emission and Reflection Radiometer (ASTER) instrument has been observing the Earth's surface at high spatial resolution and in multiple wavelength bands during the day and night and at different times of the year (Yamaguchi *et al.* 1998). ASTER is the first commercial satellite instrument to return such data, and in particular the only one to acquire multiple wavelength bands in the thermal infrared (TIR) region. This region is critical for most geoscientists working on surface processes and lithological mapping because the energy emitted from the surface is sensitive to most of the major rock forming and alteration minerals (*e.g.*, Clark 2004). In addition, surface temperature can be extracted from these data, which is fundamental to most volcanological and ecological studies. Although ASTER is the first instrument of its kind in space, TIR data collection is not new, with much of the previous research being done from airborne instruments (Kahle 1987, Hook *et al.* 1994, Ramsey *et al.* 1999). This chapter explores some of the practical applications of TIR data in both the laboratory and remotely acquired environments. It focuses on ASTER in particular, but also mentions other systems and the caveats of moving from laboratory-based hypotheses to real world data. Two primary examples or case studies are given that highlight TIR applications to eolian and volcanological processes. These are taken from past and present studies by the author and are by no means inclusive of all the possible scientific analysis possible with TIR data. However, they do illustrate several key concepts: (1) the application of a data extraction model in two different ways; (2) the use of airborne versus spaceborne data; and (3) the extraction of both temperature and emissivity from the data.

Thermal infrared remote sensing has been used as a tool to address a variety of geologic problems such as eolian sediment transport, volcanic landform interpretation, and detailed lithologic mapping (Gillespie *et al.* 1984, Abrams *et al.* 1991, Hook *et al.* 1994, Ramsey *et al.* 1999). In the context of geological studies, this feature corresponds to the vibrational frequencies of the Si-O and C-O bonds, making TIR remote sensing excellent for the study of silicate and carbonate rocks (Lyon 1965, Hunt 1980, Salisbury and Walter 1989). Further, unlike reflection in the visible/near infrared (VNIR) portion of the spectrum, TIR spectra have been shown to be linearly additive, allowing the spectra to be interpreted as a linear mixture of its components or end-members (Thomson & Salisbury 1993, Ramsey 1996, Ramsey & Christensen 1998, Christensen *et al.* 2000, Bandfield *et al.* 2002).

Mixing of emitted energy from natural surfaces occurs at all scales. For surface units larger than the fundamental resolution (pixel) of the data, identification and mapping are commonly straight forward. The resolution of an instrument is a function of the instantaneous field of view (IFOV) and the height of the instrument above the surface. After calibration for instrument and atmospheric effects, spectra from these pixels will have similar features that allow simple classification-based algorithms to identify the extent of these regions. Examples of this style of mixing would be areas of vegetation, rock outcrops, and water bodies that are homogenous over many pixels. However, where individual components are smaller than the instrument resolution, sub-pixel mixing occurs. This style of mixing could be linear or non-linear and encompasses the collection and averaging of emitted energy by the remote sensing instrument from all surface components within any given pixel. What defines a component or end-member is up to the interpretation and needs of the scientist

examining the data. Areas of sparse vegetation where the plant size is smaller than the pixel, and rock or soil exposures that are themselves mixtures of individual minerals, would both be typical examples. This intimate mixing takes place over much of an average TIR image and produces pixel-integrated spectra that vary in relation to the percentage of each end-member present. For cases such as these, a more complex data extraction model is required in order to positively identify the presence and amount of a particular end-member within a TIR scene.

BACKGROUND

TIR principles

A fundamental goal of any remotely sensed measurement, whether in the laboratory or from space, is to determine the physical and chemical characteristics of the object under study. Depending on the wavelength region examined, properties of geologic interest can include surface roughness, mineralogy, temperature, particle size, and/or elemental abundance. The wavelength region chosen will depend on the surface property of interest as well as the availability of an instrument acquiring data in that region. Further, an understanding of the energy-matter interactions unique to each wavelength region allows development and refinement of theoretical models designed to extract parameters of interest to a scientist. In quantitative remote sensing, the user must be aware of the physics of those energy-matter interactions as well as the spectral features that result. However, that level of detail may not be warranted for other studies using remote sensing. For example, a plant biologist might care more about the primary productivity of the vegetation in a study area and not the position of the near infrared (NIR) chlorophyll reflection peak, and a geologist might be more interested in the percentage of potassium feldspar in a rock outcrop and not how the TIR absorption band morphology is affected by a thin coating of desert varnish.

Energy emitted from a surface in the thermal infrared region (6-50 µm) can be described by the Planck Equation (King *et al.* 2004a). Perfectly emitting surfaces called blackbodies have no wavelength-dependent absorption bands. Near-perfect blackbodies can be fabricated and used in laboratory instrument calibration (Ruff *et al.* 1997). Naturally occurring near-blackbody emitters are also present and arise from the scattering of the emitted energy (*i.e.*, from tightly spaced tree canopies). However, most materials do not behave as blackbodies. Rather, they have spectra with emissivity values less than one at discrete wavelengths. Commonly called absorption bands because they correspond to peaks in absorption spectra, these features are signatures of the object or mineral being analyzed (Fig. 8-1). The wavelengths corresponding to the largest absorption bands (reststrahlen bands) are present in silicate and carbonate minerals (Salisbury and Wald 1992, Salisbury 1993).

Quantitative TIR remote sensing

In order to extract the position, shape, and magnitude of these absorption bands in the TIR, one must take into account: (1) the interaction of that energy with other materials on the surface, (2) the passage of that energy through the intervening atmosphere, and (3) the capture and recording of that energy by the instrument detectors. All of these can obscure the data and introduce artifacts that must be removed. Absorption and scattering by water vapor, carbon dioxide, and stratospheric ozone in the Earth's atmosphere cause most of the TIR region to be obscured (King *et al.* 2004a). The exception is the window from 8-12 µm, which has approximately 80-90% transmission. Fortuitously, this region also corresponds to both the maximum energy emitted by the Earth (at its average global surface temperature) and the region where most silicate minerals have unique absorption bands (Fig, 8-1).

Unlike other wavelength regions, photon-matter interaction in the TIR combines linearly because of the high absorption coefficients of the minerals relative to other wavelength regions (Gillespie 1992, Adams *et al.* 1993, Ramsey & Christensen 1998). This linearity is caused by the dominance of surface or Fresnel reflection, which is governed by geometric optics (*e.g.*, light reflected from a mirror). Photons have a much shorter path length relative to the particle size and interact only once after being emitted or reflected from particles. Therefore these photons either reach the detector containing information about that particular particle, or they are quickly absorbed after being scattered, never reaching the detector. In other words, the

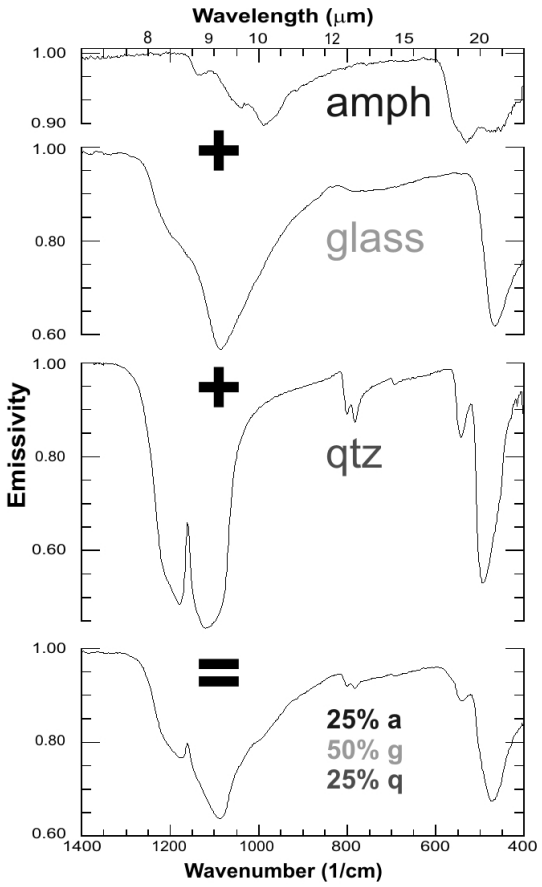

Fig. 8-1. Thermal infrared (TIR) emission spectra of two common rock-forming minerals (amphibole and quartz) as well as amorphous rhyolitic glass. The prominent emissivity lows between 8-12 μm are the fundamental vibration frequency (reststrahlen bands) of the samples. This is also the region of the prominent atmospheric window. TIR spectral features combine linearly in proportion to their areal abundance, which is the basis for the spectral deconvolution algorithm described.

detected energy is a function of the areal percentage of the end-members present. As a result, the majority of the energy detected by a sensor has interacted with only one surface particle. Upon mixing, the spectral features from surface particles are retained in proportion to their areal extent (Fig. 8-1). Therefore, if the pure mineral spectra (end-members) are known, TIR spectra can be linearly deconvolved in order to ascertain those end-member percentages (Thomson & Salisbury 1993, Ramsey & Christensen 1998, Ramsey & Fink 1999, Hamilton, 2003). Mineral identification and mapping of natural materials using this approach is simplified due to the linear nature of emitted energy in most cases. However, even in this wavelength region, the assumption of linearity becomes invalid for non-isothermal surfaces or very fine grained materials (Gillespie 1992, Ramsey & Christensen 1998, Ramsey & Dehn, 2004).

This approach can be used on a mixed sample spectrum derived from a laboratory measurement to estimate the end-member percentages as well as a root-mean-squared (RMS) error, which describes the model's ability to fit the data. Where applied to an image, the deconvolution model results in one image per end-member along with the RMS error image. Whereas the end-member images can be used to visualize spatial patterns and mixing, the RMS image becomes invaluable in order to assess the quality of a given algorithm iteration.

In addition to being able to control environmental variables such as the atmosphere and temperature, data collected in the laboratory also benefit from being collected over smaller spot sizes (typically <5 cm) with known orientations. This allows for precise measurements to be made and for the ability to account for effects such as coatings and mineral orientations or percentage variations in rocks. However, there arise certain scaling issues between laboratory and remote sensing measurements. These must be accounted for, prior to the application of any quantitative analyses using models such as linear deconvolution. The first and most obvious is contributions from the atmosphere. Even data collected in the high transmission windows are still subjected to absorption and scattering from atmospheric gases and aerosols. TIR data can be "corrected" for this attenuation by several means including theoretically based atmospheric scattering models, the collection of ground-based data at the time of image acquisition, or the use of a known calibration target within the scene. The most commonly used approach is that of a rigorous atmospheric model that uses average profiles of atmospheric species based on the time of year and the location on image. One such correction algorithm is the MODTRAN atmospheric model using a standard mid-latitude summer profile (Berke *et al.* 1989).

Upon atmospheric correction, the calibrated surface radiance is reduced to a combination of the temperature and emissivity. These data must be further reduced in order to compare the surface emissivity (a function of the material properties) with reference data such as laboratory spectra. For example, data collected by a TIR imaging instrument in six TIR spectral bands will contain seven unknowns for each pixel (spectrum): the surface brightness temperature of the pixel and one emissivity value for each of the six bands. This dependency is described by the Planck equation, but the set of equations is underdetermined with respect to physical measurements of temperature and radiance. In the laboratory, sample temperature can be measured or derived uniquely, but for a remote sensing situation this is not possible. Therefore, some assumption must be made and there are numerous approaches and models to best approximate this assumption (Realmuto 1990, Hook *et al*. 1992, Kahle *et al*. 1991). Perhaps the most straight forward approach is simply to assume an emissivity for one of the wavelength bands, derive the surface temperature using the Planck equation, and then use that derived temperature to solve the Planck equation for the remaining unknown emissivity values (Kahle *et al*. 1991). A slightly more rigorous and accurate approach is described by Realmuto (1990). This approach involves two solutions of the Planck equation per pixel using an assumed emissivity value. But unlike the previous example of assigning that assumed emissivity value to one band, this approach is free to assign it to the band with the highest derived surface temperature. In other words, for the six band image example above, the Planck equation would be solved six times for temperature for each pixel. The band with the highest derived temperature is assumed to be the one with the highest emissivity (the assumed input value). That derived temperature is then used to solve the Planck equation again to derive the five remaining emissivity values for each pixel. More complicated approaches try to account for spectral shape, radiance emitted from the atmosphere onto the surface, and surface scattering interactions. However, these approaches commonly use the technique described above as a core to the model and account for more subtle variations (*e.g.,* Hook *et al*. 1992, Gillespie *et al*. 1998).

In order to test how well a given emissivity-temperature separation algorithm works

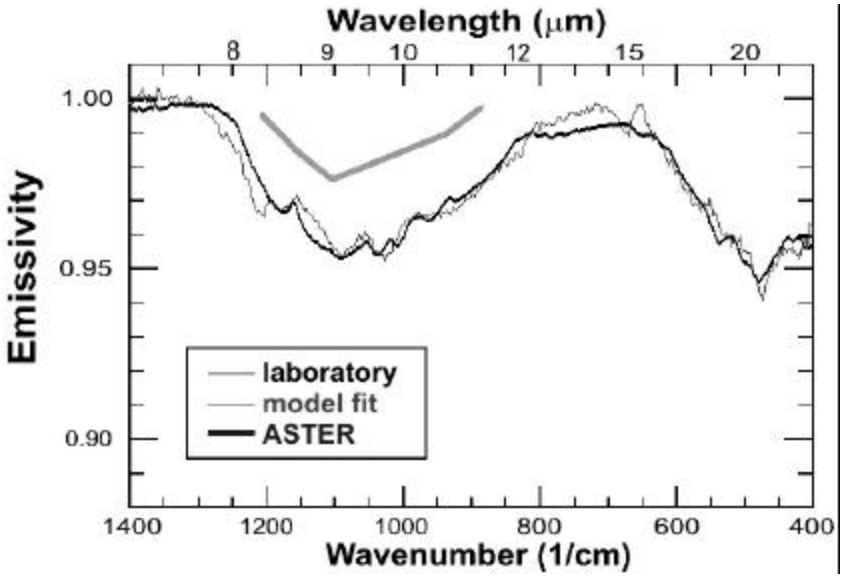

Fig. 8-2. Example of the deconvolution fit of laboratory mineral spectra to the spectrum of an andesite sample from Black Peak caldera, Alaska. The modeling approach determined the bulk mineralogy as: plagioclase = 37.9%; amphibole = 25.3%; clinopyroxene = 13.5%; montmorillonite = 17.5%; quartz = 5.9%. Also shown is the 5-point emissivity spectrum of the surface derived from the ASTER instrument. Note the relative agreement in shape, but offset in emissivity (see text).

or how appropriate a linear deconvolution model is to natural surfaces, one can compare laboratory and remotely acquired spectra of the same sample (Fig. 8-2). Spectra derived from remote sensing instruments of natural rock surfaces commonly show more blackbody behavior than a laboratory spectrum of a sample from the same rock surface. How can this be the case if emissivity is a non-variant property of the constituent minerals? There are several complications where comparing the laboratory and image-derived emissivity, not the least of which is incomplete accounting for the atmosphere. Most models are very generalized and local atmospheric conditions could be markedly different during the day of the data collection. Another complication related to atmospheric correction is an incomplete accounting for the downwelling radiance term. Downwelling radiance is energy absorbed by the atmosphere and re-emitted at the wavelength being detected by the remote sensing instrument. This energy will be reflected off the surface and become integrated into the total energy acquired for that pixel. However, because reflected TIR energy is the converse of the emitted TIR energy ($R = 1 - \varepsilon$) the downwelling energy where added to the emitted energy will produce the effect of driving the emissivity toward values closer to unity. This is not a critical issue for most applications because the downwelling radiance is generally small and therefore affects the derived emissivity spectra by several percent. However, where very quantitative emissivity is required, this additive energy must be considered.

In addition to incomplete removal and accounting for the atmosphere, there are several other possible complications that will produce image-derived spectra different from those derived in the laboratory. One such situation is the non-isothermal behavior of the surface covered by one pixel. If a pixel surface contains thermal shadows or small regions of elevated temperatures, the overall emitted energy will no longer be described by inverting the Planck equation. In fact, the energy is a mixture of Planck curves and the derived emissivity using an isothermal temperature assumption will have a slope imparted whose magnitude is a function of the temperature difference and the areal percentage of those temperatures. Another complication is that emitted energy from natural surfaces is a sum of energy from the minerals of interest, plus energy from the rock coatings (*i.e.,* varnish and lichen), soil cover, scattering due to surface roughness elements, and numerous other phenomena. All of these minor additions to the derived emissivity spectrum also drive the overall spectrum more toward that of a blackbody. There are numerous ways of accounting for this discrepancy between the laboratory and field, including matching of the laboratory and field spectrum, using a blackbody as an end-member in a deconvolution approach, and examining the spectral feature itself and ignoring the overall magnitude of the spectrum (*e.g.,* continuum removal) (Ramsey & Fink 1999, Hamilton, 2003, Clark 2004; Swayze, 2004).

One can either focus on surfaces that are not as prone to the aforementioned complications or use those complications to derive other fundamental parameters of the surface. The two case studies detailed in the sections below highlight both of these possibilities. In the first example, actively saltating sand dunes are examined. These provide an excellent target for TIR remote sensing because they generally lack thermal shadows and vegetation and consist of larger particles. Further, every major mineral commonly found in sand dunes (silicates, carbonates and sulfates) have diagnostic absorption features in the 8-12 μm wavelength region, making detection much easier. The use of thermal infrared remote sensing and a deconvolution approach to mineral mapping can be combined to identify more accurately dune composition and sediment transport into the system. In the second example, TIR emissivity data from an active lava dome is examined also using the deconvolution approach. Thermal variations on the surface clearly occur and do affect the derived emissivity spectrum. However, in regions where there are not large thermal fluxes, the deconvolution approach is used to estimate the amount of blackbody energy coming from the surface. This is used as a proxy for the vesicularity of the lava surface, which in turn can be used to understand the evolution and hazard state of the lava dome.

INSTRUMENTS

TIR imaging has been limited in the past, with ASTER currently being the only commercially available instrument now providing moderate spectral and moderately high spatial resolution in the TIR. This past dearth in TIR data was in part

caused by the expense of launching and maintaining large, actively cooled TIR detector arrays. Larger arrays are more expensive to fabricate, increase the complexity of calibration, and have a higher probability of failure of one or more detectors. Further, whereas the active cooling of these arrays produces a good signal to noise ratio (SNR), it also consumes large amounts of power. However, there are promising new technologies for TIR data collection at relatively low costs from orbit. One such technology is the use of uncooled thermal infrared microbolometer detectors with an acceptable SNR. The use of microbolometers allows for the production of smaller, less-expensive instruments, and eliminates the need for coolers. This technology is currently operational, being used to collect orbital TIR data of the Martian surface (Christensen *et al*. 2003).

Despite the relative lack of TIR data compared to other wavelength regions, its use, viability, and potential for geological applications have been shown by many authors (Kahle and Goetz 1983; Gillespie *et al*. 1984; Crowley and Hook 1996; Ramsey *et al*. 1999). Platforms with the capability of thermal infrared imaging became a reality in the 1960's with the Television Infrared Observation Satellite (TIROS) meteorological satellites and continued with the short-lived Heat Capacity Mapping Mission (HCMM) in 1978. For the next two decades, only the Thematic Mapper (TM) and the Advanced Very High Resolution Radiometer (AVHRR) instruments provided reasonably-high spatial resolution thermal infrared data from Earth orbit. These instruments acquire continuous data over much of the globe, however feature interpretation is hindered by the spatial and spectral resolution. For example, TM had 120 m/pixel spatial resolution (60 metres for the Enhanced TM (ETM+) instrument on Landsat 7) with only one broadband channel between 10.5 µm and 12.5 µm. By comparison, AVHRR instruments have two channels spanning the 8-12 µm atmospheric window, but the spatial resolution is only 1.1 km/pixel (Sabins 1987).

TIMS/MASTER

The NASA airborne Thermal Infrared Multispectral Scanner (TIMS) instrument is no longer operational, but collected data from 1981 to 1996. It was designed to operate within the 8-12 µm atmospheric window, collecting six spectral bands of high spatial resolution radiant energy from the ground surface and intervening atmospheric column (Kahle and Goetz 1983; Palluconi and Meeks 1985). The spatial resolution of each image pixel was dependent on the aircraft altitude and instrument field of view. The TIMS also served as the first simulator for the ASTER instrument and these data still provide the only high spatial resolution TIR data for many areas. (Kahle *et al*. 1991, Yamaguchi *et al*. 1998, Abrams 2000).

The TIMS instrument was replaced by the more advance airborne MODIS/ASTER simulator (MASTER) instrument, which was developed to simulate and validate ASTER and MODIS (Moderate Resolution Imaging Spectroradiometer) data (Hook *et al*. 2001). The MASTER instrument collects reflected and emitted energy over 50 channels from the VNIR to the TIR region. There are eleven bands in the VNIR region, twenty nine in the short wave-mid infrared (SWIR/MIR) region, and ten in the TIR region. It has an identical instantaneous field of view (IFOV) as TIMS (2.5 mrad). Typically flown on the Department of Energy (DOE) King Air Beechcraft B200, this combination results in spatial resolutions of 5 to 25 m/pixel depending on surface and flight altitude.

MTI

The Multispectral Thermal Imager (MTI) is a space-based research and development project sponsored by the DOE and the Office of Nonproliferation and National Security. MTI's primary objective is to demonstrate advanced multispectral and thermal imaging, image processing, and associated technologies that could be used in future systems for detecting and characterizing facilities producing weapons of mass destruction. The MTI system consists of a single satellite in a polar, 360-mile-high orbit carrying an advanced sensor capable of imaging 15 spectral bands from the VNIR to the TIR region. There are four bands in the VNIR (5 m/pixel), eight in the SWIR/MIR (20 m/pixel), and three in the TIR (20 m/pixel). MTI data are not publicly available, but can be provided as part of the MTI Users Group, which consists of scientists conducting non-classified research.

ASTER

The Advanced Spaceborne Thermal Emission and Reflectance Radiometer (ASTER) instrument was launched on the Terra satellite in December 1999 as part of the NASA Earth Observing System (EOS). It is one of five sensors on the Terra satellite and designed to acquire repetitive, high spatial resolution, multi-spectral data from the VNIR to the TIR region – the first time for any commercial satellite (Yamaguchi *et al.* 1998, Abrams, 2000). It comprises three separate subsystems operating with three channels in the VNIR (15 m/pixel) region, six channels in the short wave infrared (SWIR) region (30 m/pixel), and five channels in the TIR (90 m/pixel) region.

The Terra platform follows a sun-synchronous, polar orbit slightly over 30 minutes behind the Landsat 7 satellite providing ASTER with a nominal repeat time of 16 days. However, at higher latitudes this number drops to less than 7 days. In addition, ASTER has a unique cross-track pointing capability of up to 24° off axis, allowing image collection up to ±85º latitude. This side-looking ability can further decrease repeat acquisition time to several days at high latitudes, however it lowers spatial resolution and increases the atmospheric path length. In addition to its broad spectral coverage and pointing ability, the instrument can generate along-track digital elevation models (DEMs) using one backward-looking telescope in the VNIR (Welch *et al.* 1998, Abrams 2000). The resulting DEMs have a posting of 30 metres and are optically generated using the parallax between the two images. Finally, ASTER data are acquired using one of several dynamic ranges in order to mitigate data saturation (over highly reflective targets such as snow and ice) and low signal to noise (over minimally reflective targets, such as water). All of these unique properties of the ASTER sensor are providing new tools with which to monitor small-scale changes in surface processes. Unfortunately, because ASTER is an experimental instrument, there are no future plans to extend the technology of spaceborne multispectral thermal IR for Earth observations.

CASE STUDY: EOLIAN PROCESSES

In the world's arid and semi-arid regions, eolian processes such as sediment weathering, transport, and deposition are constantly ongoing within active sand pathways. The analysis of dune field composition and sand movement are critical for the interpretation of past climatic conditions, the local geology, and assessing future desertification hazards such as land degradation and dust storm initiation. Sand movement on active dunes and reactivation of existing vegetation-stabilized sand surfaces have been shown to increase the albedo (the average reflectance over a given wavelength region) of desert areas, with important local and regional impacts on climate, and to increase significantly dust emissions from desert surfaces. Further, this sand movement impacts human settlements and agriculture, making desertification a significant hazard to nearly 25% of the world's population. In order to perform a comprehensive study on the temporal dynamics of a single eolian system requires many years of data collection, mapping, and sample classification (*e.g.*, Sharp 1966, Muhs *et al.* 1995). Detailed field studies of this nature are extremely valuable. However, the large amount of time required versus the small area that can be analyzed can clearly lead to generalizations in both the source and amount of mineralogic heterogeneity within a large dune field. Such assumptions result in errors that propagate through subsequent models.

Remote sensing offers a more comprehensive tool to study dynamic features such as dunes and has given the geologist a synoptic view of entire eolian systems and sources (Breed & Grow 1979, Blount *et al.* 1990, Ramsey *et al.* 1999). In addition, the ability to examine changes over time allows for the extrapolation of past climatic regimes and the monitoring of marginal areas susceptible to future desertification (Leonidov 1989, Tucker *et al.* 1994). Past workers have looked at the visible-near infrared (VNIR) reflectance and overall albedo as proxies for activity (Paisley *et al.* 1991). However, to approach the level of detail needed to track specific sediment transport paths, information below the scale of the image resolution, such as the surface mineralogy and abundance, are critical (Ramsey *et al.* 1999, Bandfield *et al.* 2002). One such approach used successfully for active sand transportation studies is the application of a linear spectral deconvolution approach to multispectral remote sensing data. In the past, spectral deconvolution using TIR data has been attempted on both felsic (quartz- and feldspar-rich) sands (Ramsey *et al.*

1999) as well as mafic (iron- and magnesium-rich) dunes (Bandfield *et al.* 2002). Results of both studies clearly identified surface mineralogy as well as mixing patterns of the components.

The focus here is a summary of a study carried out at the Kelso Dunes located in the Mojave Desert, California (Ramsey *et al.* 1999). That work used field, laboratory, and airborne image analyses to determine new source inputs into the dune field. Those more localized sources implied a younger age for a large percentage of the sediment and contradicted aspects of previous field-based studies, which documented an older more stabilized sand transport pathway (Sharp 1966, Lancaster 1993). The results of that work are then compared to new work using a similar approach on TIR data from the ASTER instrument.

The Kelso Dunes, CA

Located approximately 95 km west of the Colorado River in southern California, the core of the Kelso Dunes covers over 100 km^2. It consists of a region of active sand transportation with three large parallel linear ridges up to 170 m high. However, the overall westward migration of the dunes is kept to a minimum by topographically controlled winds, which oppose the prevailing easterly wind direction (Sharp 1966, Reheis & Kihl 1995). The dune field is contained within a topographic basin, encroaching upon alluvial fans to the south and east (Plate 8-1). During previous more arid periods the primary sand source was the outwash of the Mojave River to the west (Smith 1984). However, under the current climate regime active long-distance sand transport is limited and Ramsey *et al.* (1999) hypothesized that local sediment sources such as the alluvial fans may provide the primary source of new input into the dunes.

Airborne TIMS data were acquired on 12 June 1995 at 21 m/pixel spatial resolution and cover the entire active dune field, the paleo-sand transport to the west, as well as the surrounding mountain ranges and alluvial fans (Plate 8-1). The calibrated IR radiance images were corrected for atmospheric absorption and scattering using the MODTRAN radiative transfer model (Berke *et al.* 1989). These data were then separated into six emissivity and one kinetic temperature (*e.g.*, the temperature derived from a radiance measurement using an emissivity less than 1.0) image, with the emissivity data used to model the mineralogical composition of the surface. The six-point surface emissivity spectra were compared to laboratory spectra from samples collected throughout the dune field, and were also used as input into the deconvolution model along with a spectral library of major rock forming minerals.

Samples collected throughout the active dunes and surrounding areas were also analyzed using traditional petrographic techniques including point counts of the loose sand grains under low magnification and in thin section using higher magnification. The four dominant end-members identified in the sand samples were quartz, plagioclase feldspar (primarily oligoclase), alkali feldspar (microcline), and clay (montmorillonite). In addition, a surface lag deposit of fine-grained magnetite is present locally and appeared in higher concentrations in some samples. Thermal IR laboratory spectra were collected on the same sand samples (Fig. 8-3). These spectra were compared to those derived from the TIMS data as well as subjected to the same linear deconvolution approach as the TIMS 6-point spectra. These analyses confirmed the presence of the same mineral end-members identified in the petrographic results.

An interesting result of the mineral mapping using IR emissivity data arose by examining spatial distribution of the microcline end-member (Plate 8-2). The distribution of microcline is somewhat over-predicted by the model where compared to the petrographic analyses. However, the microcline end-member image also showed a clear concentration in the active dune sand and on the alluvial fan to the east. Samples collected here contained model-identified microcline in decreasing percentages from 67% at the base of the granite outcrops to 57% at the base of the active dunes. At the crest of a series of active dunes within the field, the microcline percentage dropped to 45%. This potential local source for a major mineral constituent of the dunes had not been identified in previous studies (Sharp 1966, Lancaster 1993). Ramsey *et al.* (1999) hypothesized a transportation scenario by which the microcline, weathered out of the monzonite grus and soils present on the alluvial fans, is then incorporated into the dunes. This material is being transported into the central part of the field by fluvial activity and the intermittent

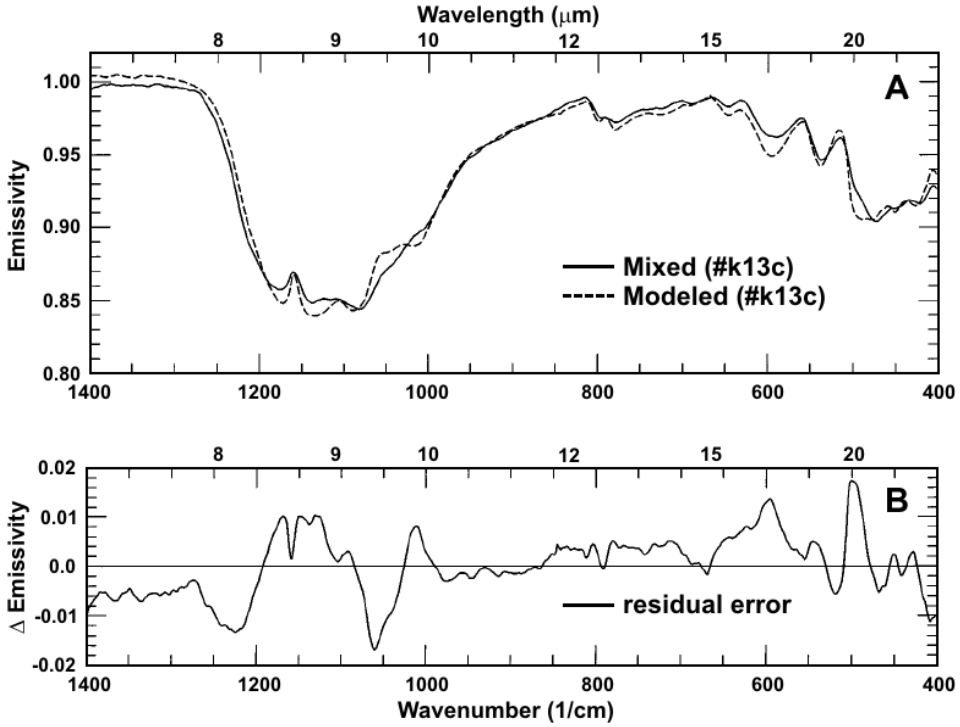

Fig. 8-3. Deconvolution model results for the laboratory spectrum of Kelso sand sample K13. **(A)** Fit using the library end-members. **(B)** The residual error (measured minus modeled) shows the regions of poor fit over the large absorption bands. These errors approach 2% at 9.5 μm and 20 μm and are due to poorly modeled feldspar features. The average root-mean-squared error for this deconvolution iteration was 0.63%, indicating a good fit. Modified after Ramsey *et al.* (1999).

orthographic winds from the east.

With the availability of spaceborne multispectral TIR data for the first time from ASTER, similar studies can be performed on eolian systems throughout the world's deserts. However, in order to apply such an approach, an understanding of the spatial and spectral degradation effects on the deconvolution model is critical. By comparison with the TIMS data of Kelso, the spatial resolution of ASTER is more than a factor of four lower and the spectral resolution drops from six to five bands.Despite these losses, the major patterns of most mineral end-members are still identifiable with ASTER (Plate 8-2). For larger eolian systems, the 90 m resolution of the TIR would not be a limiting factor. However, a major limiting factor does arise in the spectral degradation to 5 bands. The loss of the 9 μm band in ASTER because of stratospheric ozone absorption (King *et al.* 2004a) corresponds with the absorption of many feldspar minerals, including microcline. This makes the identification of the local microcline source seen with TIMS, much more problematic using ASTER. Therefore caution must be applied where using ASTER for mineral identification in eolian systems as the lack of a positive mineral identification does not guarantee its absence on the surface (Ramsey, 2002).

The formation of new eolian deposits can be strongly influenced by sediment availability that is in turn related to regional climatic changes (Wells and McFadden 1987; Lancaster 1993). In particular, drought-prone areas on the metastable margins of these transport pathways and sand seas are easily susceptible to sand encroachment, dust storms, and desertification with environmental change. For example, sand migration and encroachment onto fragile silt and clay-rich surfaces of dry lake beds (playas) in the central Chad region of the Saharan Desert have been linked to the initiation of the large trans-Atlantic dust storms. Recent research has highlighted the importance of dust storms in transporting aerosols that affect global climate

dynamics (via changes in the radiative properties of the atmosphere) as well as to human health in areas close to the source of dust in addition to far-distant populations (Cahill *et al*. 1996, Gillette 1999). Further, this sand movement impacts human settlements and agriculture, making desertification a significant hazard. Temporal studies of these dynamic systems are now being carried out in arid regions throughout the world using ASTER. Despite the aforementioned limitations, it is hoped that localized sand source regions, the distance over which the dunes migrate, and the degree to which this migration initiates the injection of dust into the atmosphere can be identified.

CASE STUDY: VOLCANOLOGIC PROCESSES

In chapter 9 some of the remote sensing approaches that can be made to examine inactive, altered volcanic edifices are discussed (Crowley *et al*. 2004). By using similar modeling techniques for multispectral IR emissivity data collected from active volcanoes, physical properties of the lava can also be extracted. These properties include surface roughness at the micrometre scale and thermal flux of the system, both of which can be critical for understanding the state of the volcanic system and its hazard potential. The linear spectral deconvolution approach described previously has been adapted for fresh lava surfaces in order to extract the percentage of glass and roughness elements at the 10 to 100 micrometre scale (Ramsey & Fink 1999, Ramsey & Dehn 2004, Byrnes *et al*. 2004). The ability to adapt the approach is plausible because of the linear behavior of emitted energy in this region as well as a different end-members set. The choice of end-members can range from minerals to lithologic units to surface pumiceous textures depending on the objective of the study and the availability of data. Textural end-members used as inputs into such a model, produce images that reveal subtle mixing patterns and allow for the areal distribution of those textures to be calculated.

Although used by several authors to analyze textures of silicic lava domes and basaltic lava flows, these earlier studies relied on airborne data of inactive flows (Ramsey & Fink 1999, Byrnes *et al*. 2000, Eisenger *et al*. 2000). Ramsey and Fink (1999) have shown that multispectral TIR emissivity can be used to estimate the percentage of vesicles (or the micron-scale roughness) on the surface of Holocene silicic domes using this approach. By modeling the emissivity spectrum derived from each pixel on the dome surface as a combination of glass and featureless blackbody emission (a proxy for vesicles and roughness elements) they showed that vesicularity could be estimated to within 5% under ideal situations (this is summarized in Chapter 4; King *et al*. 2004b). Even more importantly, it was speculated that changes in the vesicle amount and location on the dome could indicate the emplacement of new lava and the potential for further dome collapse.

With the availability of global coverage of ASTER thermal infrared (TIR) data, the possibility of applying the approach to active systems is now possible. Because ASTER is the first satellite instrument to acquire high spatial resolution, multispectral data in the thermal infrared region, together with the ability to generate coincident DEMs, the instrument is particularly useful for numerous aspects of volcanic remote sensing. The multispectral thermal infrared capability is critical for monitoring both low and high temperature thermal anomalies as well as mapping chemical and textural variations on lava surfaces. TIR remote sensing data such as those provided by ASTER are sensitive to textural, compositional, thermal, and atmospheric anomalies, and therefore provides a tool to observe and map these changes.

For most of 2000 the dome of Bezymianny Volcano, Russia, was undergoing endogenic growth and subsequent collapse, forming small-scale pyroclastic flows and ash emissions (Ramsey & Dehn 2002). ASTER data from the SWIR and TIR regions were used to monitor eruptions and map the volcanic products at Bezymianny from June 1, 2000, to January 30, 2001. The work described here summarizes that of Ramsey & Dehn (2004), who applied the deconvolution technique for the first time to the study of an active silicic dome. The results of that work are then compared to new data from more recent eruptions and highlight the utility of having both a high temporal and low spatial resolution monitoring system (*i.e*., AVHRR) coupled with a low temporal and high spatial resolution instrument (*i.e*., ASTER).

Bezymianny Volcano, Russia

Bezymianny is an andesitic to dacitic stratovolcano lying on the southern end of the

Kliuchevskoi group of volcanoes (Plate 8-3). Following the large debris-avalanche eruption in March 1956, Bezymianny has been one of the most historically active volcanoes on the Kamchatka Peninsula, producing dome-forming eruptions and less-common large ash plumes (Gorshkov 1959). On average, Bezymianny has nearly two eruptive cycles per year typically in the form of unrest at the lava dome. As new material is extruded, periods of fracture and collapse follow that can produce sub-Plinian eruption columns as well as block and ash flows into the valleys to the east and south of the volcano (Fedotov & Masurenkov 1991). Although the population surrounding the volcano is sparse and not in direct threat from its eruptions, Bezymianny does pose a significant hazard to air traffic flying the north Pacific routes. Approximately 25,000 people (more than 100 passenger flights) and 1 billion dollars (U.S.) in cargo and equipment fly over this region each day (Miller and Casadevall 2000). Therefore, the Alaska Volcano Observatory (AVO) together with the Kamchatka Volcano Eruption Response Team (KVERT) monitor these volcanoes from space using primarily polar-orbiting, high temporal resolution instruments like AVHRR (Dehn *et al*. 2000).

During 2000, Bezymianny entered a period of enhanced activity punctuated by several larger eruption sequences. Fourteen cloud free ASTER scenes acquired at night show obvious thermal anomalies covering tens to hundreds of pixels and reveal both the eruptive and quiescent behavior of the volcanic dome and small to moderate-size pyroclastic flows. The derived level-2 ASTER standard data products (kinetic temperature and emissivity) were examined for the scenes of the volcano and the surrounding area. Throughout the summer observation period between the larger eruptions of March and October, every ASTER TIR image showed some level of increased thermal output on the dome complex (Plate 8-4).

The extent of the warmer pixels changed dramatically over the entire nine months of ASTER data collection, indicating a dynamic condition during endogenic dome growth (Plate 8-4). The movement is most likely controlled by the availability of surface water and the creation of new fractures during dome growth. The thermal activity during this time could also represent normal dome activity at Bezymianny, or the final stages of the March 2000 eruptive cycle. Regardless, such anomalies could never before be measured with such precision from space. The high radiometric accuracy of the ASTER TIR subsystem coupled with 90 m pixels allows for a 1-2°C detection threshold. For all the anomalies during the summer period, the temperature range was 2-15°C above the average background.

The ASTER emissivity data also have been used to map textural variations on the active lava dome. The same observation dates were subjected to the deconvolution model using a laboratory-derived silica-rich obsidian glass spectrum and the spectrum of a blackbody as end-members. This represents the first time this approach has been applied to an actively-erupting silicic dome. The roughness results for the model were color coded and showed variation from 2% to 74%, with an average value of approximately 40% (Plate 8-4). Statistically significant low (<20%) and high (>60%) values were present on the dome and surrounding talus slopes, appearing to be concentrated in the regions of highest thermal anomalies. Although potentially the result of non-linear temperature mixing, the extracted emissivity spectra over these hot pixels clearly show variability not related to temperature. The correlation of that variability with other volcanic eruptive processes is the focus of continued research (Kuhn & Ramsey 2003).

High-resolution data such as ASTER are critical for volcanic studies in that they allow for the discrimination of smaller thermal, textural, and compositional anomalies on the surfaces of lava flows and domes. However, even during eruptions where ASTER is in an increased acquisition mode, the repeat time (several day average) is not sufficient for its use strictly as a monitoring tool. For that objective, a higher temporal frequency (minutes to hours) instrument must be utilized. However, data from such instruments clearly fail to capture any of the small-scale eruption activity or the nominal non-eruptive character of these remote volcanoes. The combination of a high temporal, low spatial and spectral resolution instrument and a low temporal, high spatial and spectral resolution instrument provides the ideal data set for observation of the large scale eruptive trends and the small scale volcanic processes. To achieve this integrated strategy, a newly-funded NASA proposal will utilize data from the AVHRR monitoring effort as a trigger

for ASTER emergency data requests, thereby providing ASTER data to the AVO analyst within 1-2 days after collection. In preparation for this new infrastructure, current eruptions of Bezymianny and other Kamchatka volcanoes are immediately communicated to NASA for ASTER scheduling and acquisition. This verbal and email approach results in significant delays that will be reduced with the future automated system. However, even the current cooperation is resulting in excellent ASTER data coverage that captured new pyroclastic flow deposits, a new exogenous lobe emplacement, and new thermal features (Fig. 8-4).

CONCLUSIONS

Vibrational spectroscopy may be used to detect the fundamental, combination, and overtone frequencies of the molecules in mineral or amorphous substances of geologic interest. More specifically, the absorbed energy at shorter wavelengths is emitted as thermal flux at longer wavelengths by way of the atomic bond and crystal lattice vibrations. Because of this process, the detection of these vibrational frequencies or absorption bands relates fundamental information on the mineralogy itself. Knowing the mineralogy of a rock or alluvial surface is critically important to a geologist trying to interpret the geologic, climatic, or volcanic history of the surface. Newly developed mapping tools and identification algorithms such as linear deconvolution provide an extension of that mapping ability, allowing for sub-pixel abundances to be quantitatively determined. This approach has also served as the basis for assessing a scale of roughness on lava surface similar to vesicularity, which further expands the applicability of TIR data beyond mineral mapping remote sensing.

In this synthesis paper, one common technique (spectral deconvolution) was highlighted and applied to two very different geologic processes. At the Kelso Dunes, airborne TIR data originally provided the impetus for the sample collection and initiated the petrographic analysis of the sand mineralogy. However, it was not until the development and application of the linear retrieval model that examination of specific mineral distributions became possible. The study of Ramsey *et al.* (1999) represented a rigorous attempt to quantify and validate the linear mixing assumption of thermal emission spectra for an active geologic surface. The results showed clear mineralogical variations throughout the dunes and that the field on average contains 40-50% quartz, significantly less than previous work had stated. It also identified potentially new source areas for the sand, which had implications for the regional climate of the past.

More recent work at active silicic volcanic domes was also highlighted here and focused on new ASTER data over Bezymianny Volcano in Russia. The ASTER data from April 2000 to January 2001 revealed thermal anomalies covering tens to hundreds of pixels. These data record the eruptive activity by showing the movement of anomalies with a concentration along a fissure prior to larger eruptions of October-November. That eruption was also detected by AVHRR and resulted in the formation of a hot flow deposit seen in the subsequent months by ASTER. This represents the first time such an instrument was used for a dedicated long term observation of active lava dome processes. High resolution data such as ASTER are critical for volcanic studies in that they allow for the discrimination of smaller thermal, textural, and compositional anomalies on the surfaces of lava flows and domes. In order to capture these processes in a more timely way, a new program of satellite integration is now underway. The proposed research will rely on the current satellite monitoring program of AVO to continue locate and target future eruptions transmitting that information directly to the ASTER scheduling system.

Spectroscopy and remote sensing in the TIR region has lagged behind that of other wavelength regions for numerous reasons. However, the utility of TIR remote sensing for geology and mineralogy has become clear in the past decade and numerous air- and space-based instruments have become available. The current lack of plans to extend the technology of spaceborne multispectral thermal IR for Earth observations beyond ASTER threatens a significant discontinuity in the flow data and expansion of its analyses. Therefore, even though ASTER is the first instrument to have such a capability and is proving to be an extremely valuable tool for numerous scientific studies including volcanic and eolian processes, it may be the last of its kind for many years.

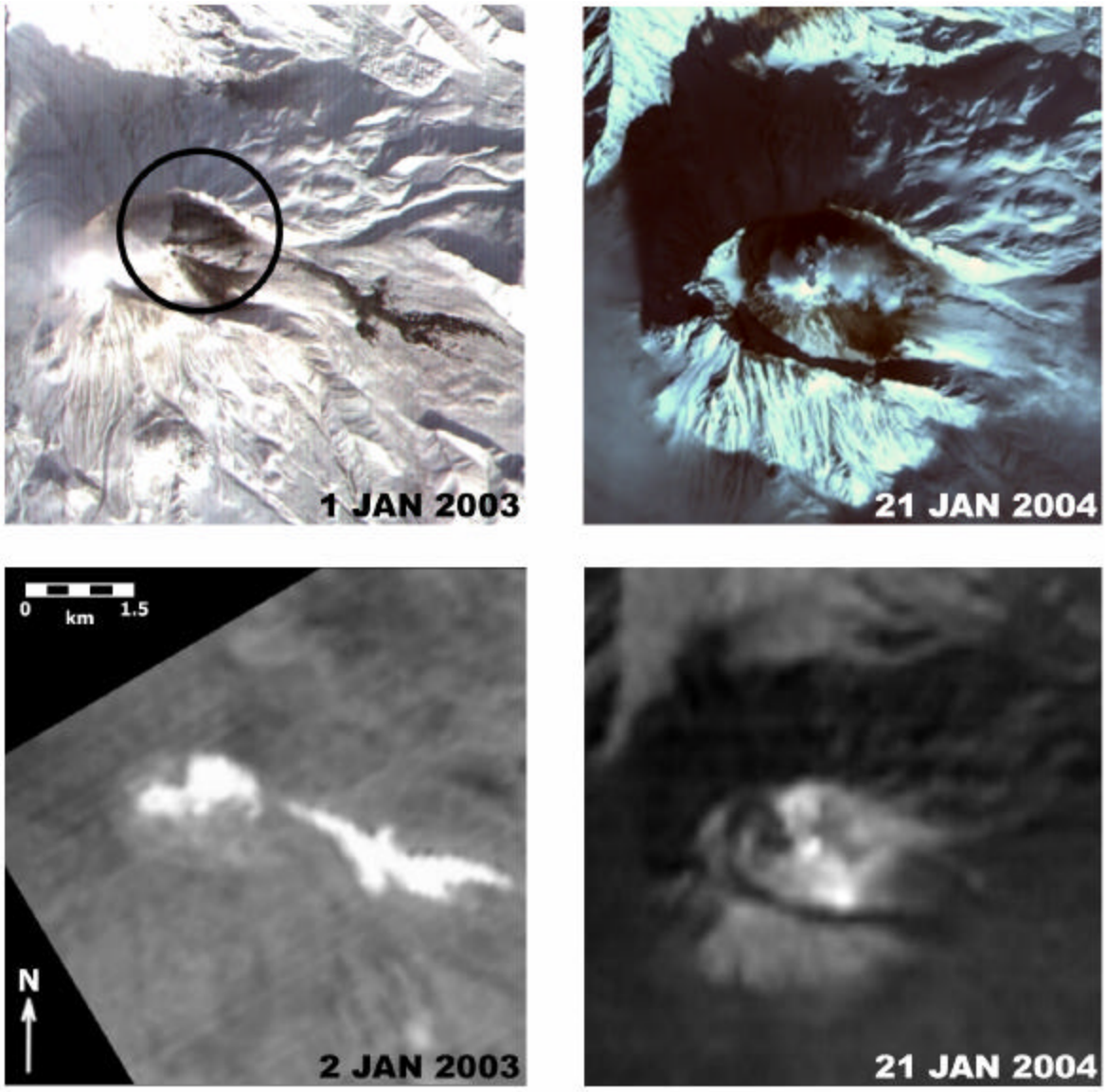

Fig 8-4. ASTER data captured during recent eruptive phases of Bezymianny Volcano. These data were collected following detection of thermal anomalies during routine monitoring by the AVO using the AVHRR instrument. Upon detection, ASTER was then placed in an "urgent acquisition" mode and data acquired during the next possible overpass (1-4 days). The ASTER VNIR data are shown at the top and the TIR data below. The January 2003 data reveal a new lobe was extruded onto the dome (circle) and a debris avalanche deposited to the east. These features are also clearly evident in the TIR data. The January 2004 data were collected following a series of eruptions producing larger ash plumes. However, no significant thermal anomaly is present, nor a large surface deposit visible.

ACKNOWLEDGEMENTS

I would like to thank Ken Edgett (Kelso Dunes research), as well as Rick Wessels and Olga Girina (Bezymianny Volcano research) for numerous discussions and their assistance in the field. In addition, the co-authors on the original manuscripts provided important science direction and assistance with those studies: Philip Christensen, Douglas

Howard, and Nick Lancaster (Kelso Dunes); Jonathon Dehn (Bezymianny Volcano). The quality of this manuscript was greatly improved thanks to helpful reviews by Michael Abrams, Ken Dean, and Penny King. Research funding for this study has been provided by NASA through the Solid Earth and Natural Hazards Program (NAG5-9438 and NAG5-9439) as well as the ASTER Science Project.

REFERENCES

ABRAMS, M.J., ABBOTT, E. & KAHLE, A.B. (1991): Combined use of visible, reflected infrared, and thermal infrared images for mapping Hawaiian lava flows. *J. Geophys. Res.* **96**, 475-484.

ABRAMS, M. (2000): The Advanced Spaceborne Thermal Emission And Reflectance Radiometer (ASTER): Data products for the high spatial resolution imager on NASA's Terra platform. *Int. J. Rem. Sens.* **21**, 847-859.

ADAMS, J.B., SMITH, M.O. & GILLESPIE, A.R. (1993): Imaging spectroscopy: Interpretation based on spectral mixture analysis. In *Remote Geochemical Analysis: Elemental and Mineralogical Composition* (eds. PIETERS, C.M. & ENGLERT, P.A.), Cambridge University Press, New York, NY, 145-166.

BANDFIELD, J.L., EDGETT, K.S. & CHRISTENSEN, P.R. (2002): Spectroscopic study of the Moses Lake dune field, Washington: Determination of compositional distributions and source lithologies. *J. Geophys. Res.* **107**, 5092, doi:10.1029/2000JE001469.

BERKE, A., BERNSTEIN, L.S. & ROBERTSON, D.C. (1989): MODTRAN: A moderate-resolution for LOWTRAN 7: Air Force System Command. *Geophysical Laboratory Report GL-TR-89-0122.*

BLOUNT, G., SMITH, M.O., ADAMS, J.B., GREELEY, R. & CHRISTENSEN, P.R. (1990): Regional aeolian dynamics and sand mixing in the Gran Desierto: Evidence from Landsat Thematic Mapper images. *J. Geophys. Res.* **95**, 15463-15482.

BREED, C.S. & GROW, T. (1979): Morphology and distribution of dunes in sand seas observed by remote sensing. In *A study of global sand seas: U.S. Geological Survey Professional Paper* (ed. MCKEE, E.D.) Vol 1052, 253-301.

BYRNES, J.M., CROWN, D.A. & RAMSEY, M.S. (2000): Thermal remote sensing characteristics of basaltic lava flow surface units: Implications for flow field evolution, *Lunar Planet. Sci. Conf. XXXI (CD-ROM), Abs. 1867*.

BYRNES, J.M., RAMSEY, M.S. & CROWN, D.A. (2004): Emplacement of the Mauna Ulu flow field, Kilauea Volcano, Hawaii: New insights from ASTER and the MASTER airborne simulator. *J. Volc. Geotherm. Res., (in press)*.

CAHILL, T.A., GILL, T.E., REID, J.S. GEARHART, E.A.& GILLETTE, D.A. (1996): Saltating particles, playa crusts, and dust aerosols at Owens (Dry) Lake, California. *Earth Surf. Proc. and Landforms* **21**, 621-640.

CHRISTENSEN, P.R., BANDFIELD, J.L., SMITH, M.D., HAMILTON, V.E. & CLARK, R.N. (2000): Identification of a basaltic component on the Martian surface from Thermal Emission Spectrometer data. *J. Geophys. Res.* **105**, 9609-9622.

CHRISTENSEN, P.R. & 21 OTHERS (2003): Morphology and composition of the surface of Mars: Mars Odyssey THEMIS results. *Science* **300**, 2056-2061.

CLARK, R.N. (2004): Spectroscopy of rocks and minerals, and principles of spectroscopy. *In* Molecules to Planets: Infrared Spectroscopy in Geochemistry, Exploration Geochemistry and Remote Sensing (P.L. King, M.S. Ramsey, G.Swayze, eds.). Mineral. Assoc. Canada, Short Course **33**, xxx-xxx.

CROWLEY, J.K. & HOOK, S.J. (1996): Mapping playa evaporite minerals and associated sediments in Death Valley, California, with multispectral thermal infrared images. *J Geophys. Res.* **101**, 643-660.

CROWLEY, J.K., MARS, J.C., JOHN, D. A., MUFFLER, L.J.P. & CLYNNE, M.A. (2004): Hydrothermal Mineral Zoning Within an Eroded Stratocone: Remote Sensing Spectral Analysis of Brokeoff Volcano, California. *In* Molecules to Planets: Infrared Spectroscopy in Geochemistry, Exploration Geochemistry and Remote Sensing (P.L. King, M.S. Ramsey, G.Swayze, eds.). Mineral. Assoc. Canada, Short Course **33**, xxx-xxx.

DEHN, J., DEAN, K.G. & ENGLE, K. (2000): Thermal monitoring of North Pacific volcanoes from Space. *Geology* **28**, 755-758.

EISINGER, C.L., RAMSEY, M.S., WESSELS, R.L. & FINK, J.H. (2000): Discriminating compositional variations on the silicic domes of Medicine Lake Volcano, CA, with the new airborne hyperspectral MODIS/ASTER simulator. *Abstr. of the Gen. Assembly IAVCEI*, p. 158.

FEDOTOV, S.A. & MASURENKOV, Y.P. (1991): *Active Volcanoes of Kamchatka volume 1*. Nauka Publishers, Moscow, 301 p.

GILLESPIE, A.R., KAHLE, A.B. & PALLUCONI, F.D. (1984): Mapping alluvial fans in Death Valley, California, using multichannel thermal infrared images. *Geophys. Res. Let., 11*, 1153-1156.

GILLESPIE, A.R. (1992): Spectral mixture analysis of multispectral thermal infrared images. *Remote Sens. Environ.* **42**, 137-145.

GILLESPIE, A.R., MATSUNAGA, T., ROKUGAWA, S. & HOOK, S.J. (1998): Temperature and emissivity separation from Advanced Spaceborne Thermal Emission and Reflection Radiometer (ASTER) images. *IEEE Trans. Geosci. Rem. Sens.* **36**, 1113-1126.

GILLETTE, D.A. (1999): A Qualitative geophysical explanation for "hot spot" dust emitting source regions. *Contrib. Atmos. Phys.* **72**, 7-77.

GORSHKOV, G.S. (1959): Gigantic eruption of Bezymianny Volcano. *Bull. Volcanologique* **20**, 77-109.

HAMILTON, V.E. (2003): Thermal infrared emission spectroscopy of titanium-enriched pyroxenes. *J. Geophys. Res.* **108**, doi:10.1029/2003JE002052.

HOOK, S.J., GABELL, A.R., GREEN, A.A. & KEALY, P.S. (1992): A comparison of techniques for extracting emissivity information from thermal infrared data for geologic studies. *Rem. Sens. Environ.* **42**, 123-135.

HOOK, S.J., KARLSTROM, K.E., MILLER, C.F. & MCCAFFREY, K.J.W. (1994): Mapping the Piute Mountains, California, with Thermal Infrared Multispectral Scanner (TIMS) Images. *J. Geophys. Res.* **99**, 15605-15622.

HOOK, S.J., MYERS, J.J., THOME, K.J., FITZGERALD, M. & KAHLE, A.B. (2001): The MODIS/ASTER airborne simulator (MASTER) – a new instrument for Earth science studies. *Rem. Sens. Environ.* **76**, 93-102.

HUNT, G.R. (1980): Electromagnetic radiation: The communication link in remote sensing. *In* Remote Sensing in Geology (SIEGEL, B.S. & GILLESPIE, A.R., eds.) John Wiley, New York, (5-45).

KAHLE, A.B. & GOETZ, A.F.H. (1983): Mineralogic information from a new airborne thermal infrared multispectral scanner. *Science* **222**, 24-27.

KAHLE, A.B. (1987): Surface emittance, temperature, and thermal inertia derived from thermal infrared multispectral scanner (TIMS) data for Death Valley, California. *Geophys.* **52**, 858-874.

KAHLE, A.B., PALLUCONI, F.D., HOOK, S.J., REALMUTO, V.J. & BOTHWELL, G. (1991): The advanced spaceborne thermal emission and reflectance radiometer (ASTER). *Inter. J. Imaging Sys. Tech.* **3**, 144-156.

KAHLE, A.B. & ALLEY, R.E. (1992): Separation of temperature and emittance in remotely sensed radiance measurements. *Rem. Sens. Environ.* **42**, 107-111.

KING, P.L., RAMSEY, M.S., MCMILLAN, P. F. & SWAYZE, G. (2004a): Instrumentation and methods in Fourier transform infrared spectrosocopy with application to geologic samples. *In* Molecules to Planets: Infrared Spectroscopy in Geochemistry, Exploration Geochemistry and Remote Sensing (P.L. King, M.S. Ramsey, G.Swayze, eds.). Mineral. Assoc. Canada, Short Course **33**, xxx-xxx.

KING, P.L., MCMILLAN, P. F. & MOORE, G. (2004b): Infrared Spectroscopy of Silicate Glasses with Application to Natural Systems. *In* Molecules to Planets: Infrared Spectroscopy in Geochemistry, Exploration Geochemistry and Remote Sensing (P.L. King, M.S. Ramsey, G.Swayze, eds.). Mineral. Assoc. Canada, Short Course **33**, xxx-xxx.

KUHN, S.S. & RAMSEY, M.S. (2003): Growth of the Soufriere Hills Dome: Fusion of Thermal Infrared Spaceborne Data with a Multi-parameter Database. *Third Cities on Volcanoes Mtg. Abs. Vol., p. 21.*

LANCASTER, N. (1993): Development of the Kelso Dunes, Mojave Desert, California, *Nat. Geog. Res. Explor*. **9**. 444-459.

LEONIDOV, V.A. (1989): Remote sensing of reclaimed lands and adjacent territories in the fight against desertification. *Prob. Desert Develop*. **3**, 46-59.

LYON, R.J.P. (1965): Analysis of rocks by spectral infrared emission (8 to 25 microns). *Econ. Geol*. **60**, 715-736.

MILLER, T.P. & CASADEVALL, T.J. (2000): Volcanic ash hazards to aviation. In *Encyclopedia of Volcanoes* (Sigurdsson, H., Houghton, B., McNutt, S.R., Rymer H. & Stix, J., eds.), Academic Press, New York, NY (915-930).

MUHS, D.R., BUSH, C.A., COWHERD, S.D. & MAHAN, S. (1995): Source of sand for the Algodones Dunes. In *Desert Aeolian Processes* (Tchakerian, V.P., ed.), Chapman and Hall, New York, NY, 37-74.

PAISLEY, E.C.I., LANCASTER, N., GADDIS, L.R. & GREELEY, R. (1991): Discrimination of active and inactive sand from remote sensing: Kelso Dunes, Mojave Desert, California. *Rem. Sens. Environ*. **37**, 153-166.

PALLUCONI, F.D. & MEEKS, G.R. (1985): Thermal infrared multispectral scanner (TIMS): An investigators guide to TIMS data. *JPL Publ. 85-32*, 1-14.

RAMSEY, M.S. (1996): Quantitative analysis of geological surfaces: A deconvolution algorithm for midinfrared remote sensing data. *Ph.D. dissertation, Ariz. State Univ.*, Tempe, AZ, 1-276.

RAMSEY, M.S. & CHRISTENSEN, P.R. (1998): Mineral abundance determination: Quantitative deconvolution of thermal emission spectra. *J. Geophys. Res.* **103**, 577-596.

RAMSEY, M.S. & FINK, J.H. (1999): Estimating silicic lava vesicularity with thermal remote sensing: A new technique for volcanic mapping and monitoring. *Bull. Volc.* **61**, 32-39.

RAMSEY, M.S., CHRISTENSEN, P.R., LANCASTER, N. & HOWARD, D.A. (1999): Identification of sand sources and transport pathways at the Kelso Dunes, California using thermal infrared remote sensing. *Geol. Soc. Amer. Bull.* **111**, 646-662.

RAMSEY, M.S. (2002): Ejecta distribution patterns at Meteor Crater, Arizona: On the applicability of lithologic end-member deconvolution for spaceborne thermal infrared data of Earth and Mars. *J. Geophys. Res.* **107**, doi:10.1029/2001JE001827.

RAMSEY, M.S. & DEHN, J. (2002): The 2000 eruption of Bezymianny Volcano captured with ASTER: A proposal to integrate high-resolution remote sensing data into real-time eruption monitoring at AVO. In *Proc. of the 3rd Ann. Subduction Processes in the Kurile-Kamchatka-Aleutian Arcs*, 44-45.

RAMSEY, M.S. & DEHN, J. (2004): Spaceborne observations of the 2000 Bezymianny, Kamchatka eruption: The integration of high-resolution ASTER data into near real-time monitoring using AVHRR. *J. Volc. Geotherm. Res., (in press)*.

REALMUTO, V.J. (1990): Separating the Effects of Temperature and Emissivity: Emissivity Spectrum Normalization. *In* Proc. of the Second TIMS Workshop, Abbott, E.A. (ed.) JPL Pub. 90-55, JPL, Pasadena, Calif., 26-30.

REHEIS, M.C. & KIHL, R. (1995): Dust deposition in Southern Nevada and California 1984-1989: Relations to climate, source area, and lithology. *J. Geophys. Res.* **100**, 8893-8918.

RUFF, S., CHRISTENSEN, P.R., BARBERA, P.W. & ANDERSON, D.L. (1997): Quantitative thermal emission spectroscopy of minerals: A laboratory technique for measurement and calibration. *J. Geophys. Res.* **102**, 14899-14913.

SABINS, F.F. (1987): *Remote Sensing Principles and Interpretation, 2nd ed.* W.H. Freeman, New York, NY, 1-449.

SALISBURY, J.W. & WALTER, L.S. (1989): Thermal infrared (2.5-13.5 μm) spectroscopic remote sensing of igneous rock types on particulate planetary surfaces. *J. Geophys. Res.* **94**, 9192-9202.

SALISBURY, J.W. & WALD, A. (1992): The role of volume scattering in reducing spectral contrast of reststrahlen bands in spectra of powdered minerals. *Icarus* **96**, 121-128.

SALISBURY, J.W. (1993): Mid-infrared spectroscopy: Laboratory data, in *Remote Geochemical Analysis: Elemental and Mineralogical Composition* (eds. PIETERS, C.M. & ENGLERT, P.A.), Cambridge University Press, New York, NY, 79-98.

SHARP, R.P. (1966): Kelso Dunes, Mojave Desert, California, *Geol. Soc. Amer. Bull.* **77**, 1045-1074.

SMITH, R.S.U. (1984): Eolian geomorphology of the Devils Playground, Kelso Dunes and Silurian Valley, California. In *Surficial Geology of the Eastern Mojave Desert, California* (ed. Dohrenwend J.C.), Geological Society of America, Boulder, CO, 162-173.

SWAYZE, G.A. (2004): Using reflectance spectroscopy to evaluate minerals of environmental concern. *In* Molecules to Planets: Infrared Spectroscopy in Geochemistry, Exploration Geochemistry and Remote Sensing (P.L. King, M.S. Ramsey, G.Swayze, eds.). Mineral. Assoc. Canada, Short Course **33**, xxx-xxx.

THOMSON, J.L. & SALISBURY, J.W. (1993): The mid-infrared reflectance of mineral mixtures (7-14 μm). *Rem. Sens. Environ.* **45**, 1-13 1993.

TUCKER, C.J., NEWCOMB, W.W. & DREGNE, H.E. (1994): AVHRR data sets for determination of desert spatial extent. *Int. J. Rem. Sens.* **15**, 3547-3456.

WELCH, R., JORDAN, T., LANG, H. & MURAKAMI, H. (1998): ASTER as a source for topographic data in the late 1990's. *IEEE Trans. Geosci. Rem. Sens.* **36**, 1282-1289 1998.

WELLS, S.G. & MCFADDEN, L.D. (1987): Influence of Late Quaternary climatic changes on geomorphic processes on a desert piedmont, eastern Mojave Desert, California. *Quatern. Res.* **27**, 130-146 1987.

YAMAGUCHI, Y., KAHLE, A.B., TSU, H., KAWAKAMI, T. & PNIEL, M. (1998): Overview of the Advanced Spaceborne Thermal Emission And Reflectance Radiometer (ASTER). *IEEE Trans. Geosci. Rem. Sens.* **36**, 1062-1071.

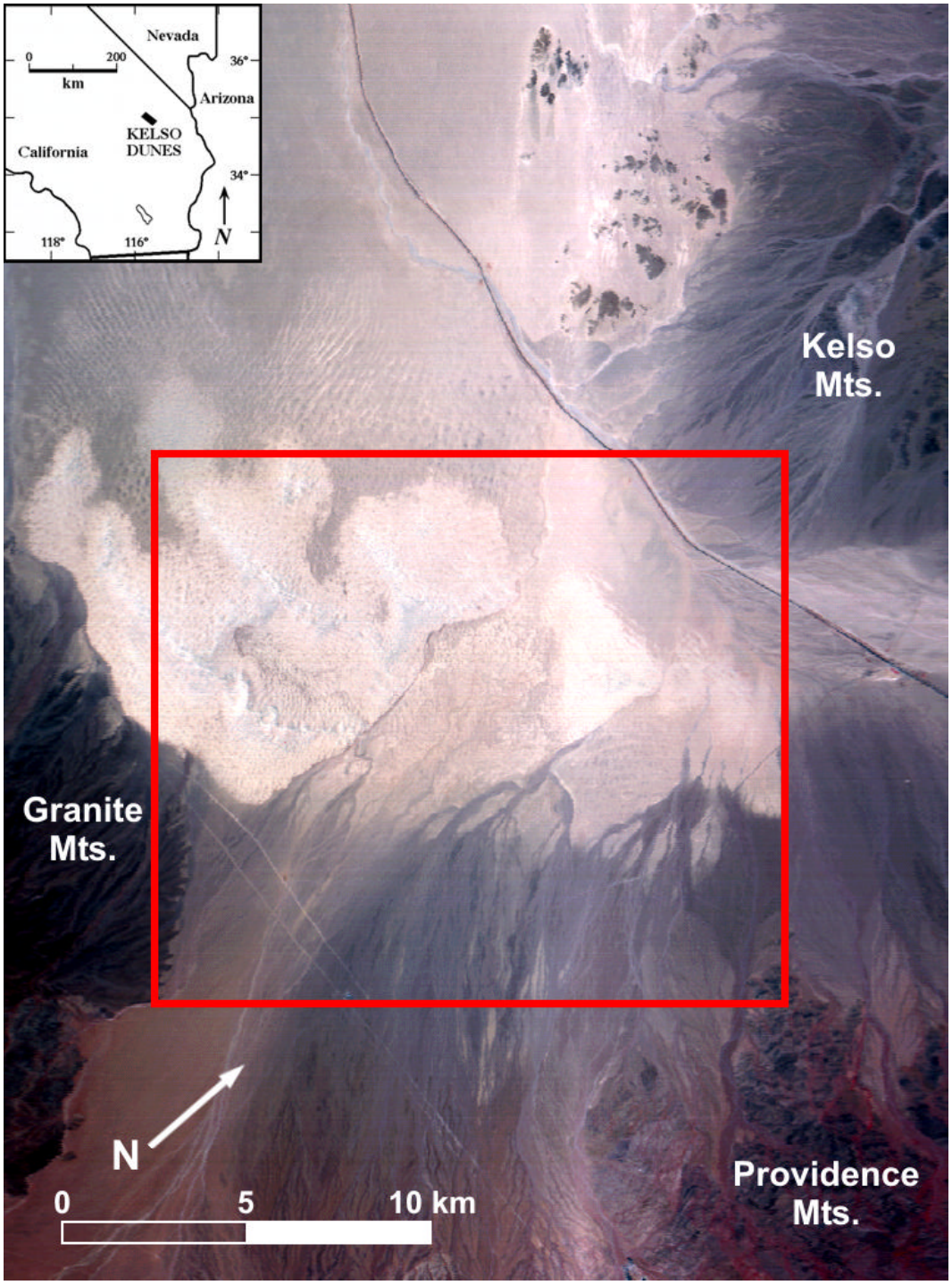

Plate 8-1. Visible wavelength airborne scanner image of the primary Kelso Dunes sand transport pathway, acquired concurrently with the Thermal Infrared Multispectral Scanner (TIMS) data in 1995. The white dashed region denotes the area analyzed in detail using the TIMS data (see Figures 5). Inset shows the location map of the Kelso Dunes in the Mojave Desert. Modified after Ramsey *et al.* (1999).

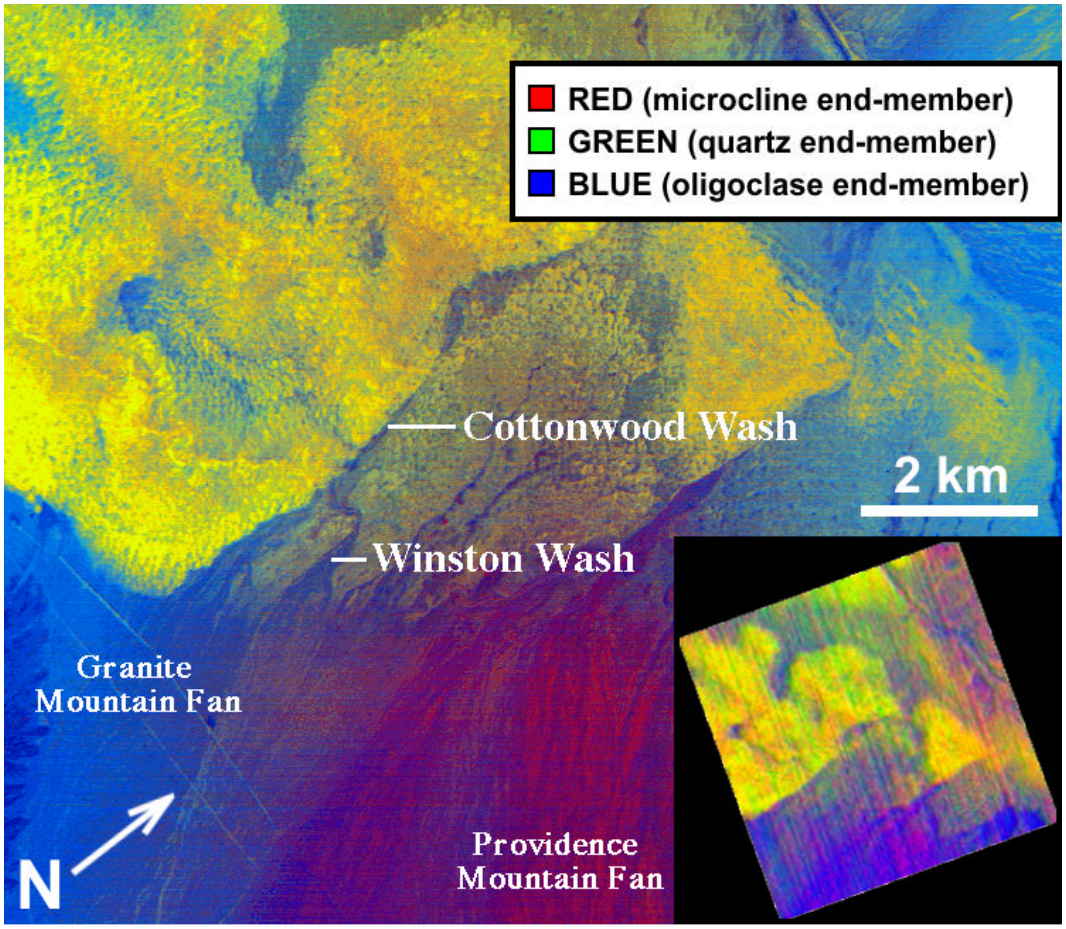

Plate 8-2. False-color composite for the TIMS data of the Kelso Dunes, showing microcline in red, quartz in green, and oligoclase in blue. Yellow indicates an nearly equal abundance of quartz and microcline, whereas cyan is quartz + oligoclase. Microcline, entering from the eastern fan of the Providence Mountains, appears to have been transported over the Cottonwood and Winston Washes and incorporated into the active dunes. Oligoclase is being derived from the northern and southern alluvial fans, and in addition occurs to a lesser extent from the west. Inset shows an ASTER-derived deconvolution result for the same mineral end-members. The image has been rotated to match the TIMS data and left at the 90 m spatial scale (compared to the 21 m/pixel scale of the TIMS data). The lower prevalence of red in the ASTER image indicates less microcline has been identified. This underdetermination is a function of the lower spatial resolution as well as the lack of the 9 µm channel on ASTER, due to stratospheric ozone absorption in this region. Modified after Ramsey *et al.* (1999).

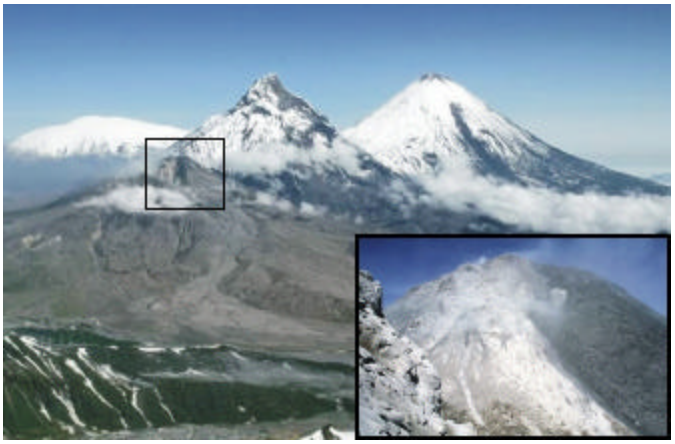

Plate 8-3. 10August 2001 view looking north-northwest to the Kliuchevskoi Volcanic Group showing Bezymianny (indicated by the box) and its associated pyroclastic deposits in the foreground.Alsovisiblenorthand to the right of Bezymianny are Kliuchevskoi and Ushkovsky Volcanoes, respectively. Inset shows the Bezymianny dome with the new (2001) lava flow. *(photographscourtesyofMichael Zelenski).*

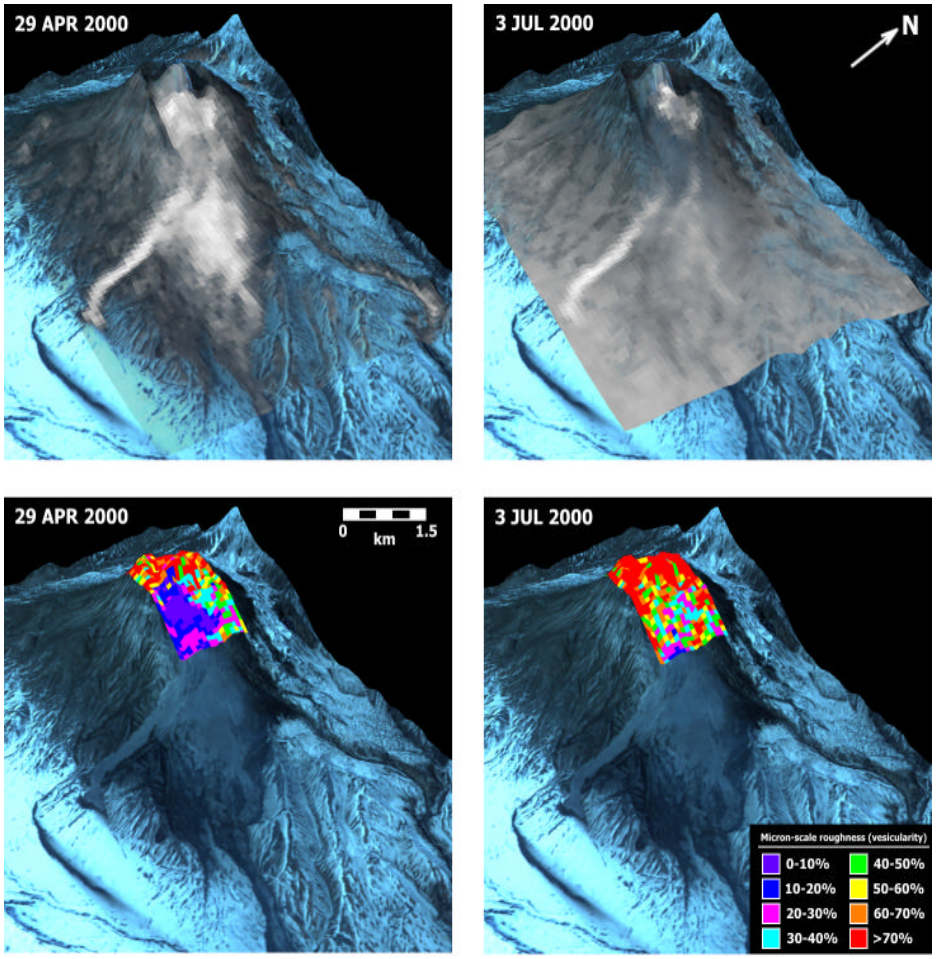

Plate8-4. ASTERderivedtemperatureandvesicularityproductsofBezymiannyfortwodatesin 2000. ASTERTIR90mpixelshavebeenoverlainonthe15m/pixelVNIRimagefromMay, 2000,whichinturnisdrapedoverthedigitalelevationmodel(DEM)fromMay,2000. Significantchangesinintensityandlocationofthethermally-elevatedpixelscanbeseenonthe dome.Followingthelargereruptionin March,2000numeroushotdebrisflowswereemplaced inthesmallvalleytothesouth. Belowthetoppanelsarethederivedvesicularity/micron-scale roughnessmaps(seetext)forthesamedates. Notethevariablemodelresultsintheregion correspondingtothehighestthermalanomaly.Thisregionofthedomeissubjecttolavaandgas emissionandtheinitiationsiteoftheobservedhotflowdeposits.ModifiedafterRamseyand Dehn(2004).